Article
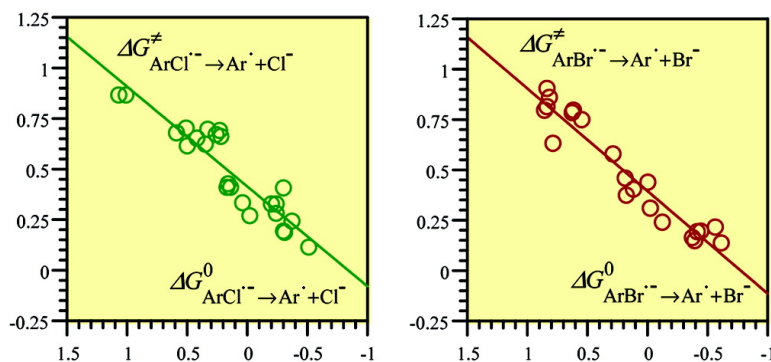
Fragmentation of Aryl Halide Anion Radicals. Bending of the Cleaving Bond and Activation vs Driving Force Relationships

Cyrille Costentin, Marc Robert, and Jean-Michel Savant

More About This Article

Additional resources and features associated with this article are available within the HTML version:

- Supporting Information
- Links to the 4 articles that cite this article, as of the time of this article download
- Access to high resolution figures
- Links to articles and content related to this article
- Copyright permission to reproduce figures and/or text from this article

View the Full Text HTML

Fragmentation of Aryl Halide π Anion Radicals. Bending of the Cleaving Bond and Activation vs Driving Force Relationships

Cyrille Costentin, Marc Robert, and Jean-Michel Savéant*

Contribution from the Laboratoire d'Electrochimie Moléculaire, Unité Mixte de Recherche Université—CNRS No. 7591, Université de Paris 7—Denis Diderot, 2 place Jussieu, 75251 Paris Cedex 05, France

Received July 6, 2004; E-mail: saveant@laposte.net

Abstract: Recent rate data for very fast cleaving of aryl chloride and bromide anion radicals may be accommodated satisfactorily within rate constant versus ArX/ArX·⁻ standard potential existing correlations provided the standard potential is determined experimentally. Cyclic voltammetry is used for this purpose, taking careful account of the electron transfer/fragmentation reaction mixed character of the kinetics. The ensuing activation/driving force relationships allow the determination of the intrinsic barriers, the magnitude of which are discussed in the framework of a new Morse curve model that includes and emphasizes the role of bond bending.

Introduction

Injection of an electron into an aromatic molecule greatly diminishes the strength of carbon-substituent bonds. The ensuing expulsion of an anion, or more generally of a nucleophile, and formation of the aryl radical is generally fast and occurs successively to the initial electron uptake in most cases (Scheme 1).[1,2]

Scheme 1

stepwise in most cases

$$ArX + e^- \rightleftharpoons ArX^{\bullet-}$$
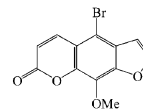
concerted

$$Ar^\bullet + X^-$$
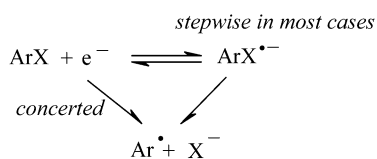
The cleavage of aromatic anion radicals has attracted considerable attention, with emphasis on the cases where the leaving group is a halide ion. Various methods have been used for the determination of the cleavage rate constant: pulse radiolysis in water,[3a−c] and nonaqueous solvents;[3d−f] direct[4] and indirect[5] electrochemistry. Another source of interest in this type of reaction is that it is involved in the propagation loop of electron-transfer catalyzed aromatic $S_{RN}1$ substitutions, whereas the reverse reaction of addition of a nucleophile to an aryl radical is the key-step of the reaction (Scheme 2).[6]

While aromatic $S_{RN}1$ reactions have given rise to a wealth of qualitative observations, kinetic data concerning the nucleophile-aromatic radical coupling[7] are less abundant than for the cleavage of aromatic halide anion radicals.

(1) (a) References 1b−1e and references therein. (b) Savéant, J.-M. *Acc. Chem. Res.* **1993**, *26*, 455. (c) Savéant, J.-M. Single Electron Transfer and Nucleophilic Substitution. In. *Advances in Physical Organic Chemistry*; Bethel, D., Ed.; Academic Press: New York, 1990, vol. 26, pp 1−130. (d) Savéant, J.-M. Electron Transfer, Bond Breaking and Bond Formation. In *Advances in Physical Organic Chemistry*; Tidwell, T., T., Ed.; Academic Press: New York, 2000, Vol. 35, pp 117−192. (e) Rossi, R. A.; Pierini, A. B.; Penenõry, A. B. *Chem. Rev.* **2003**, *103*, 71.
(2) (a) Exceptions are the electrochemical reductions of iodobenzene and 4-methyliodobenzene where the mechanism shifts from concerted to stepwise upon increasing the driving force. (b) Pause, L.; Robert, M.; Savéant, J.-M. *J. Am. Chem. Soc.* **1999**, *121*, 7158.
(3) (a) Behar, D.; Neta, P. *J. Phys. Chem.* **1981**, *85*, 690. (b) Neta, P.; Behar, D. *J. Am. Chem. Soc.* **1981**, *103*, 103. (c) Meot-Ner, M.; Neta, P. *J. Phys. Chem.* **1986**, *90*, 168. (d) Kimura, N.; Takamuku, S. *Bull. Chem. Soc. Jpn.* **1986**, *59*, 3653. (e) Kimura, N.; Takamuku, S. *Radiat. Phys. Chem.* **1987**, *29*, 179. (f) Kimura, N.; Takamuku, S. *J. Am. Chem. Soc.* **1995**, *117*, 8023.

(4) (a) Cyclic voltammetry,[4b−n] single[4o] and double potential step chronoamperometry at micro (diameter in the millimeter range) electrodes[4p] and ultra-micro (diameter in the micron range) electrodes,[4q] allowing the determination of rate constants from 10^2 to 10^7 s⁻¹. (b) Nadjo, L.; Savéant, J.-M. *J. Electroanal. Chem.* **1971**, *30*, 41. (c) Grimshaw, J.; Trocha-Grimshaw J. *J. Electroanal. Chem.* **1974**, *56*, 443. (d) Alwair, K.; Grimshaw, J. *J. Chem. Soc., Perkin Trans. 2* **1973**, 1150. (e) Gores, G. J.; Koeppe, C. E.; Bartak, D. E. *J. Org. Chem.* **1979**, *44*, 380. (f) Parker, V. D. *Acta Chem. Scand. B.* **1981**, *35*, 595. (g) Parker, V. D. *Acta Chem. Scand. B.* **1981**, *35*, 655. (h) Aalstad, B.; Parker, V. D. *Acta Chem. Scand. B.* **1982**, *36*, 47. (i) Andrieux, C. P.; Savéant J—M.; Zann, D. *Nouv. J. Chim.* **1984**, *8*, 107. (j) Andrieux, C. P.; Delgado, G.; Savéant J—M. *J. Electroanal. Chem.* **1993**, *348*, 123. (k) Chen. T.; Platz, M. S.; Robert, M.; Savéant, J.-M.; Marcinek, A.; Rogowski, J.; Gebicki, J.; Zhu, Z.; Bally, T. *J. Phys. Chem. A* **1997**, *101*, 2124. 4l (l) the structure of 5-bromo-8-methoxypsoralen studied in ref 4k is as follows:

(m) Jaworski, J. S.; Leszczynski, P.; Filipek, S. *J. Electroanal. Chem.* **1997**, *440*, 163. (n) Jaworski, J. S.; Leszczynski, P. *J. Electroanal. Chem.* **1999**, *464*, 259. (o) Danen, W. C.; Kensler, T. T.; Lawless, J. G.; Marcus, M. F.; Hawley, M. D. *J. Phys. Chem.* **1969**, *73*, 4389. (p) Andrieux, C. P.; Hapiot, P.; Savéant, J.-M. *J. Phys. Chem.* **1988**, *92*, 5987. (q) Wipf, D. O.; Wightman, M. W. *J. Phys. Chem.* **1989**, *93*, 4286.
(5) (a) That is, the redox catalysis method, the application of which allows the extension of accessible rate constants to 5×10^8 s⁻¹.[5b−e] (b) Andrieux, C. P.; Dumas-Bouchiat, J.-M.; Savéant, J.-M. *J. Electroanal. Chem.* **1978**, *88*, 43. (c) Andrieux, C. P.; Blocman, C.; Dumas-Bouchiat, J.-M.; Savéant, J.-M. *J. Am. Chem. Soc.* **1979**, *101*, 3431. (d) Andrieux, C. P.; Blocman, C.; Dumas-Bouchiat, J.-M.; M'Halla, F.; Savéant, J.-M. *J. Am. Chem. Soc.* **1980**, *102*, 3806. (e) M'Halla, F.; Pinson, J.; Savéant, J.-M. *J. Am. Chem. Soc.* **1980**, *102*, 4120. (f) A recent extension[5g] of the redox catalysis approach, using steady-state techniques or optical detection instead of cyclic voltammetry, reports the possibility to reach somewhat higher rate constants. (g) Enemaerke, R. J.; Christensen, T. B.; Jensen, H.; Daasbjerg, K. *J. Chem. Soc., Perkin Trans. 2* **2001**, 1620.

Scheme 2
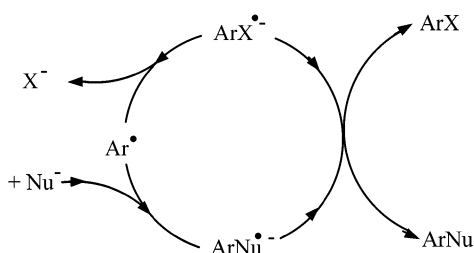
It has been observed, with chloro and bromo derivatives, that there is a rough correlation between the cleavage activation free energy and the standard potential of the ArX/ArX$^{\bullet-}$ couple.[4i] These observations prompted the development of the idea that anion radical cleavages may be viewed as intramolecular electron transfer processes,[3] more exactly as intramolecular dissociative electron-transfer processes.[8] The theory of dissociative electron transfer was consequently extended to the intramolecular case, leading to a quadratic activation driving force relationship

$$\Delta G^{\neq}_{ArX^{\bullet-}\rightarrow Ar^{\bullet}+X^-} = \Delta G^{\neq}_0 \left(1 + \frac{\Delta G^0_{ArX^{\bullet-}\rightarrow Ar^{\bullet}+X^-}}{4\Delta G^{\neq}_0}\right)^2 \quad (1)$$

$\Delta G^{\neq}_{ArX^{\bullet-}\rightarrow Ar^{\bullet}+X^-}$ is the free energy of activation and $\Delta G^0_{ArX^{\bullet-}\rightarrow Ar^{\bullet}+X^-}$, the standard free energy of cleavage, i.e., the opposite of the 'driving force'

$$\Delta G^0_{ArX^{\bullet-}\rightarrow Ar^{\bullet}+X^-} = D_{ArX\rightarrow Ar^{\bullet}+X^{\bullet}} - T\Delta S_{ArX\rightarrow Ar^{\bullet}+X^{\bullet}} + E^0_{ArX/ArX^{\bullet-}} - E^0_{X^{\bullet}/X^-} \quad (2)$$

$D_{ArX\rightarrow Ar^{\bullet}+X^{\bullet}}$ is the bond dissociation energy of the starting molecule and $\Delta S_{ArX\rightarrow Ar^{\bullet}+X^{\bullet}}$, the corresponding entropy change. The E^0 s are the standard potentials of the subscript redox couples.

The intrinsic barrier, $\Delta G^{\neq}_0$, is a function of parameters characterizing the reactant and product ground states or excited states as depicted in eqs 3−5.[8]

$$\Delta G^{\neq}_0 = \frac{D_{ArX^{\bullet-}} + \lambda_0}{4} \quad (3)$$

The cleavage reorganization energy, $D_{ArX^{\bullet-}}$, may be expressed as

$$D_{ArX^{\bullet-}} = D_{ArX\rightarrow Ar^{\bullet}+X^{\bullet}} + E^0_{ArX/Ar^{\bullet}-X^{\bullet}} - E^0_{Ar^{\bullet}/[Ar^{\bullet}]^{\bullet-}} \quad (4)$$

(see footnote 9). In $E^0_{Ar^{\bullet}/[Ar^{\bullet}]^{\bullet-}}$, $[Ar^{\bullet}]^{\bullet-}$ represents a species obtained from the injection of one electron in the π^* orbital of

the σ-radical Ar$^{\bullet}$, thus leading to an excited state of the carbanion Ar$^-$.

λ_0, the solvent reorganization energy corresponding to the transfer of the negative charge from the anion radical to the leaving halide ion, may be expressed in the Marcus way as[10]

$$\lambda_0 = \frac{e_0^2}{4\pi\epsilon_0}\left(\frac{1}{\epsilon_{op}} - \frac{1}{\epsilon_s}\right)\left(\frac{1}{2a_{ArX^{\bullet-}}} + \frac{1}{2a_{X^-}} - \frac{1}{a_{ArX^{\bullet-}} + a_{X^-}}\right) \quad (5)$$

(e_0: electron charge. ϵ_0: vacuum permittivity, ϵ_{op}, ϵ_S: solvent optical and static dielectric constants, respectively. The a's are the radii of the equivalent spheres of the subscript species).

The observed correlation observed between $\Delta G^{\neq}_{ArX^{\bullet-}\rightarrow Ar^{\bullet}+X^-}$ and $E^0_{ArX/ArX^{\bullet-}}$, for a given leaving ion, was rationalized on the following bases. In eq 2, $E^0_{X^{\bullet}/X^-}$ is the same for all members of the correlation, whereas the first two terms are approximately constant. The intrinsic barrier is likewise approximately constant, for a given halogen, which was thought as resulting from mutual compensation of the variation of the two standard potentials in eq 4.

Recent development of the field of aromatic anion radical cleavage has produced both experimental and theoretical advances. On the experimental side, improvements of the pulse radiolysis technique have allowed unprecedented access to very large cleavage rate constants, larger than 10^{10} s^{-1}.[11] These new data open the possibility of investigating a novel series of anion radicals, namely 2-, 3-, and 4-chloro and bromobiphenyl as well as 1- and 2-bromonaphthalene. This is a particularly interesting set of anion radicals since they are expected to stand at the most negative extremity of the driving force range. An estimation of the standard potentials, $E^0_{ArX/ArX^{\bullet-}}$, is needed in order to test the correlation for these new anion radicals, in the chloro and in the bromo series. While an estimate can be derived from previous redox catalysis data for 1- and 2-bromonaphthalene,[5g] this is not the case for the six chloro and bromobiphenyl. The experimental determination of these values in the biphenyl series was the first task of the work reported in this paper. All the available data will then be gathered together to examine the correlation between the activation free energy, $\Delta G^{\neq}_{ArX^{\bullet-}\rightarrow Ar^{\bullet}+X^-}$, and the driving force $\Delta G^0_{ArX^{\bullet-}\rightarrow Ar^{\bullet}+X^-}$.

The recent theoretical advance, alluded to earlier, concerns the way in which bending of the carbon−halogen bond affects the height of the activation barrier.[12] The necessity of bending the cleaving bond to relieve the orbital symmetry restriction that opposes electron transfer from the π^* to the σ^* orbitals, has been recognized for a long time.[1,6,13] The merit of the recent analyses, illustrated with the example of 4-cyano-chlorobenzene, is to provide a way for estimating the lowering in energy between the conical intersection that would be met upon straight stretching of the C−X bond and the actual bent transition state. The second purpose of this paper is to use this approach to analyze the activation/driving force relationship and its implication concerning the nature and magnitude of the intrinsic barrier

(6) (a) Limiting ourselves to *aromatic* S$_{RN}$1 substitution, key references are the following. (b) Bunnett, J. F. *Acc. Chem. Res.* **1978**, *11*, 413. (c) Savéant, J.-M. *Acc. Chem. Res.* **1980**, *13*, 323. (d) Rossi, R. A.; de Rossi, R. H. *Aromatic Substitution by the S$_{RN}$1 Mechanism*; ACS Monograph 178; American Chemical Society: Washington, DC, 1983. (e) Savéant, J.-M. *Tetrahedron* **1994**, *50*, 10117.

(7) (a) Galli, C.; Bunnett, J. F. *J. Am. Chem. Soc.* **1981**, *103*, 7141. (b) Amatore, C.; Oturan, M. A.; Pinson, J.; Savéant, J.-M.; Thiébault, A. *J. Am. Chem. Soc.* **1985**, *107*, 3451. (c) Amatore, C.; Combellas, C.; Pinson, J.; Oturan, M. A.; Robveille, S.; Savéant, J.-M.; Thiébault, A. *J. Am. Chem. Soc.* **1985**, *107*, 4846. (d) Amatore, C.; Combellas, C.; Robveille, S.; Savéant, J.-M.; Thiébault, A. *J. Electroanal. Chem.* **1985**, *185*, 25. (e) Amatore, C.; Combellas, C.; Robveille, S.; Savéant, J.-M.; Thiébault, A. *J. Am. Chem. Soc.* **1986**, *108*, 4754.

(8) Savéant, J.-M. *J. Phys. Chem.* **1994**, *98*, 3716.

(9) The two entropic terms,[8] $T(S_{ArX} - S_{ArX^{\bullet-}})$ and $-T(S_{Ar^{\bullet}} - S_{[Ar^{\bullet}]^{\bullet-}})$ may be considered as compensating each other.

(10) Marcus, R. A. Theory and Applications of Electron Transfers at Electrodes and in Solution. In *Special Topics in Electrochemistry*; Rock, P. A., Ed.; Elsevier: New York, 1977; pp 161−179.

(11) Takeda, N.; Poliakov, P. V.; Cook, A. R.; Miller, J. R. *J. Am. Chem. Soc.* **2004**, *126*, 4301.

(12) (a) Laage, D.; Burghardt, I.; Sommerfeld, T.; Hynes, J. T. *Chem. Phys. Chem.* **2003**, *4*, 61. (b) Laage, D.; Burghardt, I.; Sommerfeld, T.; Hynes, J. T. *J. Phys. Chem. A* **2003**, *107*, 11271. (c) Burghardt, I.; Laage, D.; Hynes, J. T. *J. Phys. Chem. A* **2003**, *107*, 11292.

(13) Clarke, D. D.; Coulson, C. A. *J. Chem. Soc. A* **1969**, 169.
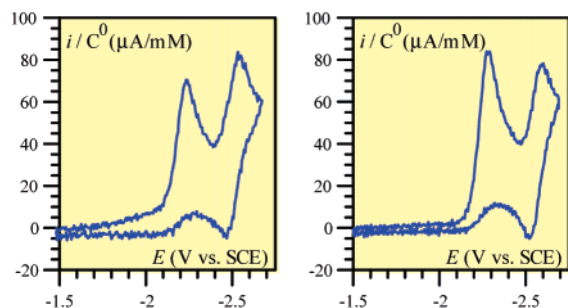
Figure 1. Cyclic voltammetry of 3-chloro-biphenyl in NMP and DMF (+ 0.1 M Bu₄NBF₄) at 22 °C. Scan rate: 0.3 V/s.
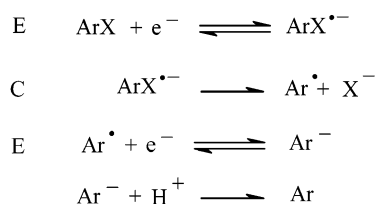
in the ArCl and ArBr series. More precisely, thanks to the determination of the standard potentials, we will examine the correlation between the experimental activation energy and thermodynamic driving force (minus the standard free energy of activation). It will then be shown that the resulting intrinsic barriers are definitely smaller than the values predicted by the classical Morse curve model of anion radical cleavage.[8] An extension of this model, which includes the effect of bond bending and of interactions between caged fragments, will then be derived, allowing one to gauge the existence and magnitude of these effects.[14]

Standard Potentials $E^0_{\text{ArX/ArX}\cdot^-}$ of Chloro- and Bromo-biphenyls. The strategy we followed consists of the derivation of the standard potential from cyclic voltammetric data, introducing in their treatment the cleavage rate constants recently obtained from pulse radiolysis.[11] The solvent used in the pulse radiolysis experiments was 1-methyl-2-pyrrolidinone (NMP) whereas N,N'-dimethylformamide (DMF) was the solvent in which previous data used for the correlation were gathered. The cleavage rate constants in the two solvents may be regarded as closely the same in view of the close similarity of their dielectric properties ($\epsilon_S = 32.2$ and 36 for NMP and DMF respectively) and of the free energies of transfer of Cl⁻ and Br⁻ from water to NMP (0.528 and 0.383 eV) and from water to DMF (0.497 and 0.394 eV), respectively.[15] The voltammograms of all six compounds exhibit an initial two-electron irreversible wave followed by a reversible one-electron wave at all accessible scan rates (a typical example is shown in Figure 1). They are almost identical in the two solvents.

The first wave corresponds to the ECE reaction sequence depicted in Scheme 3.[16a−c]

The aryl radical, Ar•, is much easier to reduce (E^0 around 0 V vs SCE)[17] than the starting ArX (E^0 in the range −2.3/−2.6 V vs SCE, see Table 1). This circumstance and the rapidity of the cleavage also rule out the possibility of a 'DISP' mechanism involving the reduction of Ar• by ArX•⁻.

---

(14) (a) Besides the case of 4-cyano-chlorobenzene, treated in details in ref 12, an indication that bond bending effects may play an important role is given in ref 11, where it is shown on the base of DFT calculations that the transition states are more bended than the initial state and that the activation energy calculated with no geometrical constraint is smaller than the activation energy with forced planarity (corresponding to a conical intersection). However, the comparison seems uncertain, if not inaccurate, since a single reference method was used in these calculations (B3LYP), as strongly emphasized in many cases when conical intersections are involved (see, for example, refs 14b−d). (b) Woywod, C.; Domcke, W.; Sobolewski, A. L.; Werner, H.-J. *J. Chem. Phys.* **1994**, *100*, 1400. (c) Robb, M. A.; Olivucci, M. *J. Photochem. Photobiol. A: Chem.* **2001**, *144*, 237. (d) *Modern Electronic Structure Theory*; Yarkony, D. R., Ed.; World Scientific: Singapore, 1995; Part 1, Chapter 2.
(15) Marcus, Y. *Ion Properties*; Marcel Dekker: New York, 1997.

Scheme 3

E   ArX + e⁻ ⇌ ArX•⁻

C   ArX•⁻ ⟶ Ar• + X⁻

E   Ar• + e⁻ ⇌ Ar⁻

     Ar⁻ + H⁺ ⟶ Ar

Table 1. Fragmentation Rate Constants and Standard Potential of the Initial Electron Transfer

biphenyl	k_f (s⁻¹)[a]	$E^0_{\text{ArX/ArX}\cdot^-}$ (V vs SCE)
2-chloro	7×10^{10}	−2.59
3-chloro	7×10^{5}	−2.36
4-chloro	4.5×10^{8}	−2.43
2-bromo	$>5 \times 10^{10}$	< −2.55
3-bromo	1.3×10^{9}	−2.38
4-bromo	3.2×10^{10}	−2.43

[a] From ref 11.

Indeed, because the cleavage is fast, Ar• is formed close to the electrode surface and it is reduced before it has time to diffuse toward the solution and react with ArX•⁻.[18] Protonation of the resulting aryl carbanion finally produces biphenyl, whose reduction gives rise to the one-electron reversible second wave, along which it is reduced to an anion radical, stable within the time window of the experiment. The second wave is expected to be the same for all the biphenyl derivatives as indeed found experimentally. The first wave is under mixed kinetic control by the first electron transfer and the follow-up cleavage reaction as attested by the slopes of the peak potential-log$v$ plot (E_p is the peak potential and v the scan rate) and by the values of the peak width ($E_{p/2}$ is the half-peak potential) shown in Figure 2.

Because of the follow-up reaction, the peak potential is more positive than the standard potential, but this positive shift is limited by the kinetic interference of electron transfer. This is characterized by a standard potential, $E^0_{\text{ArX/ArX}\cdot^-}$, a standard rate constant, k_S and a transfer coefficient, α, while the cleavage reaction is characterized by its rate constant k_f. As shown in the Supporting Information, the shape of the voltammograms is a function of a single dimensionless parameter, $(Fv/2RT)[k_f/(k_S/\sqrt{D})^4]$ (D is the diffusion coefficient), which governs the kinetic competition between electron transfer and follow-up reaction. The location of the peak potential is a function of the same competition parameter and of a potential that combines the standard potential and the rate constant of the follow-up reaction

$$E^0_{\text{ArX/ArX}\cdot^-} + \left(\frac{RT}{2F}\ln 10\right)\log(k_f)$$

The procedure for determining $E^0_{\text{ArX/ArX}\cdot^-}$, detailed in the Supporting Information, thus consists of the determination of

(16) (a) Mastragostino, M.; Nadjo, L.; Savéant, J.-M. *Electrochim. Acta* **1968**, *13*, 721. (b) Nadjo, L.; Savéant, J.-M. *J. Electroanal. Chem.* **1973**, *48*, 113. (c) Amatore, C.; Savéant, J.-M. *J. Electroanal. Chem.* **1977**, *85*, 27. (d) Andrieux, C. P.; Savéant, J.-M.; Tallec, A.; Tardivel, R.; Tardy, C *J. Am. Chem. Soc.* **1997**, *119*, 2420.
(17) Andrieux, C. P.; Pinson, J.-M. *J. Am. Chem. Soc.* **2003**, *125*, 14801.
(18) In more quantitative terms, the parameter that governs the DISP-ECE competition, $(k_{disp}/k_f^{3/2})C_0\sqrt{Fv/RT}$[16] ($k_f$, the cleavage rate constant, is taken as 10^{10} s⁻¹, k_{disp}, equal in this case to the bimolecular diffusion limit, is taken as 10^{10} M⁻¹ s⁻¹, C_0, the bulk concentration as 1 mM) ranges from 2×10^{-8} to 6×10^{-6}, i.e., is very much in favor of the ECE pathway, for an interval of scan rates, v, ranging from 0.1 to 10 000 V/s.
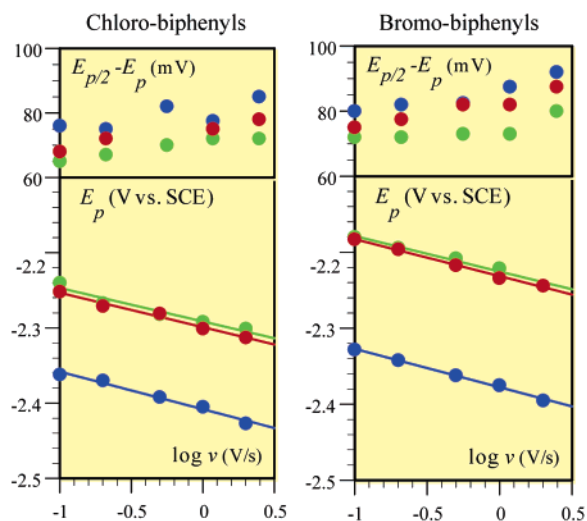
Figure 2. Cyclic voltammetry of chloro- and bromo-biphenyls in DMF (+ 0.1 M Bu_4NBF_4) at 22 °C. Peak-width and peak potentials—log v plots. blue: 2-, green: 3-, red: 4-derivative.
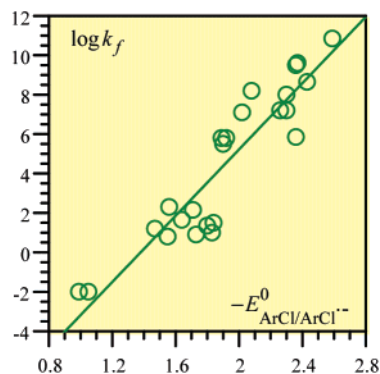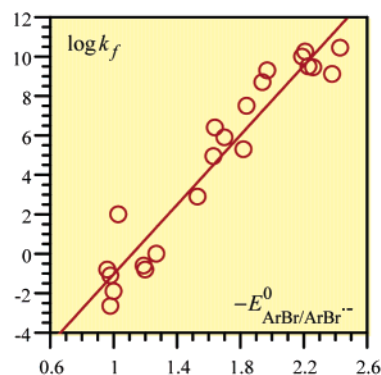

Figure 3. Correlation between the cleavage rate constants (in s^{-1}) and the standard potential for aryl chlorides (in V vs SCE). Data from Table 2.

the competition parameter from the values of the peak width, and, knowing this factor, in the derivation of the above combined potential from the values of the peak potential. Since the cleavage rate constants are known, the values of the standard potential are finally obtained (Table 1). The accuracy is ± 5 mV.

Activation/Standard Potential and Activation/Driving Force Correlations. Adding the chloro- and bromo-biphenyls data thus obtained as well as those concerning the 1- and 2-bromonaphthalene to the formerly gathered data[4i−k,5g] leads to the correlations shown in Figures 3 and 4. To help reading the rather congested diagrams in Figures 3 and 4, the rate and standard potential data are listed in Tables 2 and 3 with the appropriate references.

We see that the new members in each family fall on the correlation line with practically the same degree of scatter than the previous ones (inclusion of the biphenyl derivatives improves slightly the correlation coefficient for the bromides, which varies from 0.96 to 0.97, while it remains equal to 0.92 for the chlorides). Concerning the standard potentials of the biphenyl derivatives, it is interesting to note that the value for the 2-chloro derivative is very negative, more negative than that of biphenyl itself (-2.54 V vs SCE). This observation may be interpreted by the fact that steric hindrance resulting from the presence of the chlorine atom in an ortho-position hampers the conjugation

Figure 4. Correlation between the cleavage rate constants (in s^{-1}) and the standard potential for aryl bromides (in V vs SCE). Data from Table 3.

Table 2. Fragmentation Rate Constants and Standard Potentials for Aryl Chlorides in DMF

ArCl	log k_f (s^{-1})	$-E^0_{ArX/ArX^{\bullet-}}$ (V vs SCE)
2-chloronitrobenzene	-2.0 ± 0.1^a	0.99^a
4-chloronitrobenzene	-2.0 ± 0.1^a	1.05^a
9,10-dichloroanthracene	1.2 ± 0.1^b	1.47^b
4,4′-dichlorobenzophenone	0.8 ± 0.1^b	1.55^b
2-chlorobenzaldehyde	2.3 ± 0.1^b	1.56^b
3-chlorobenzophenone	1.65 ± 0.10^a	1.64^a
9-chloroanthracene	2.15 ± 0.03^c	1.71^a
1-chloroanthracene	0.90 ± 0.04^c	1.73^a
2-chloroanthracene	1.35 ± 0.04^c	1.80^a
3-chloroacetophenone	1.0 ± 0.1^a	1.83^a
4-[2-(4-chlorophenyl)ethenyl]-pyridine	1.5 ± 0.1^a	1.84^a
4-chloroquinoleine	5.8 ± 0.6^a	1.89^a
4′-chloroacetophenone	5.5 ± 0.6^a	1.90^a
2-chloroquinoleine	5.8 ± 0.6^a	1.92^a
ethyl 4-chlorobenzoate	7.1 ± 0.1^b	2.02^b
4-chlorobenzonitrile	8.2 ± 0.6^a	2.08^a
1-chloronaphthalene	$7.2 \pm 0.6^{a,d}$	2.26^a
2-chloronaphthalene	8.0 ± 0.6^a	2.30^a
	7.2^d	2.30^a
3-chloropyridine	9.5 ± 0.15^b	2.36^b
3-chlorobiphenyl	5.85^d	2.36^e
2-chloropyridine	9.6 ± 0.14^b	2.37^b
4-chlorobiphenyl	8.65 ± 0.02^d	2.43^e
2-chlorobiphenyl	10.85^d	2.59^e

^{a} From ref 4i. ^{b} From ref 5g. ^{c} From ref 4j. ^{d} From ref 11. ^{e} This work. ^{f} Uncertainties on standard potentials are less than 10 mV.

of the two phenyl rings thus rendering more difficult the injection of an electron into the π^* orbital. An even larger negative shift is expected with the 2-bromo derivative leading, to a rate constant too high to be measured, as predicted by the correlation.

Converting now the $E^0_{ArX/ArX^{\bullet-}}$ scale into a driving force scale by means of eq 2, we use experimental values for the two standard potentials, taking for $E^0_{ArX/ArX^{\bullet-}}$ the values just used in Figures 3 and 4 and literature values for $E^0_{X^{\bullet}/X^-}$, 1.81 and 1.42 V vs SCE in DMF for Cl and Br, respectively.[19]

(19) (a) Standard redox potentials of the $X^{\bullet}/X^-$ (X = Cl, Br) couples in DMF versus aqueous SCE were derived from the following expression: $E^{0,DMF}_{X^{\bullet}/X^-}$ (vs. SCE) = $E^{0,DMF}_{X^{\bullet}/X^-}$(vs. Ag/Ag$^+$) + $E^{0,DMF}_{Ag^+/Ag}$(vs. SCE) = $\mu^{0,DMF}_{X^{\bullet}} - \mu^{0,DMF}_{X^-} - \mu^{0,DMF}_{Ag^+} + \mu^0_{Ag} + 0.44 \approx \mu^{0,H_2O}_{X^{\bullet}} - (\mu^{0,H_2O}_{X^-} + \Delta_{trn}.G^0_{X^-,H_2O \rightarrow DMF}) - (\mu^{0,HO}_{Ag^+} + \Delta_{trn}.G^0_{Ag^+,H_2O \rightarrow DMF}) + \mu^0_{Ag} + 0.44 = E^{0,H_2O}_{X^{\bullet}/X^-}$(vs. SHE) $- E^{0,H_2O}_{Ag^+/Ag}$(vs. SHE) $- (\Delta_{trn}.G^0_{X^-,H_2O \rightarrow DMF} + \Delta_{trn}.G^0_{Ag^+,H_2O \rightarrow DMF}) + 0.44.$ Free enthalpies of transfer from water to DMF for the various ions were obtained from ref 15, while standard free enthalpies of formation for chlorine, bromine, chloride and bromide were collected from ref 19b. (b) *Handbook of Chemistry and Physics*, 82nd ed.; CRC Press: Boca Raton, Florida, 2001−2002; **5**-62 to **5**-86. (c) *Handbook of Chemistry and Physics*, 82nd ed.; CRC Press: Boca Raton, Florida, 2001−2002; **9**-74.

Table 3. Fragmentation Rate Constants and Standard Potentials for Aryl Bromides in DMF

ArBr	log k_f(s^{-1})	$-E^0_{ArX/ArX^{\bullet-}}$ (V vs SCE)
3-bromo-6-isopropylnitrobenzene	-0.8 ± 0.1^a	0.96^a
4-bromonitrobenzene	-2.65 ± 0.10^a	0.98^a
2-bromo-4-nitrotoluene	-1.1 ± 0.1^a	0.98^a
2-bromo-5-nitrotoluene	-1.9 ± 0.1^a	1.00^a
2-bromonitrobenzene	2.0 ± 0.1^a	1.03^a
3-bromofluorenone	-0.6 ± 0.1^a	1.19^a
1-bromofluorenone	-0.8 ± 0.1^a	1.20^a
4-bromo-3,5-dimethylnitrobenzene	0.0 ± 0.1^a	1.27^a
3-bromobenzophenone	2.9 ± 0.1^a	1.53^a
4-bromobenzophenone	4.95 ± 0.45^a	1.63^a
5-bromo-8-methoxypsoralen	6.4 ± 0.3^b	1.64^b
9-bromoanthracene	5.9 ± 0.6^a	1.70^a
3′-bromoacetophenone	5.3 ± 0.6^a	1.82^a
4′-bromoacetophenone	7.5 ± 0.6^a	1.84^a
4-bromobenzonitrile	8.7 ± 0.1^c	1.94^c
ethyl 4-bromobenzoate	9.30 ± 0.15^c	1.97^c
1-bromonaphthalene	10.00 ± 0.15^d	2.19^a
2-bromonaphthalene	10.25 ± 0.10^d	2.21^c
3-bromopyridine	9.50 ± 0.15^c	2.23^c
2-bromopyridine	9.45 ± 0.15^c	2.26^c
3-bromobiphenyl	9.1 ± 0.03^d	2.38^e
4-bromobiphenyl	10.45 ± 0.14^d	2.43^e

^{a} From ref 4i. ^{b} From ref 4k. ^{c} From ref 5g. ^{d} From ref 11. ^{e} This work. ^{f} Uncertainties on standard potentials are less than 10 m V.

Table 4. Computed BDE s and Entropic Terms^a

compound	$D_{ArX \rightarrow Ar^{\bullet}+X^{\bullet}}$	$T\Delta S_{ArX \rightarrow Ar^{\bullet}+X^{\bullet}}{}^b$
chlorobenzene	4.20^c	0.33_5
4-chloronitrobenzene	4.24	0.33_5
9-chloroanthracene	4.28	0.34_5
4-chlorobiphenyl	4.31	0.33_5
bromobenzene	$3.66_5{}^d$	0.33
4-bromonitrobenzene	3.71	0.33
9-bromoanthracene	3.73	0.34
4-bromobiphenyl	3.78	0.33

^{a} In eV. ^{b} At 25 °C, taking into account the fact that the standard states correspond to 1 mol per liter. ^{c} To be compared with the experimental value 4.22 eV. ^{d} To be compared with the experimental value 3.59 eV.

The remaining terms, i.e., the ArX bond dissociation energy (BDE) and the attending entropic term were estimated as follows. Given the halogen, the BDE is expected to vary little in each series. If this is true, then we may use the literature experimental values for PhCl and PhBr (4.22 and 3.59 eV, respectively).[19c] We checked the quasi-constancy of the BDE and its entropic term by means of a DFT calculation method particularly suited to the estimation of BDEs (see the methodology section). The results are reported in Table 4.

The activation free energy, $\Delta G^{\neq}_{ArX^{\bullet-} \rightarrow Ar^{\bullet}+X^-}$ is then obtained from

$$\Delta G^{\neq}_{ArX^{\bullet-} \rightarrow Ar^{\bullet}+X^-} = \frac{RT}{F}\ln\left(\frac{k_B T/h}{k_f}\right) \qquad (6)$$

The ensuing activation/driving force plots are shown in Figures 5 and 6.

Intrinsic Barrier. Accelerating Role of Bond Bending and of Other Factors. As seen in Figures 5 and 6, a clear correlation between activation and driving force is found for both aryl chloride and aryl bromide anion radicals. As noted earlier,[11] the correlations between lnk_f and the computed electron affinity that include the biphenyl derivatives have more scatter than the previously established correlations between lnk_f and the experi-
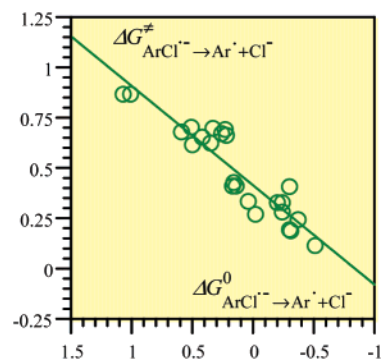
Figure 5. Activation/driving force relationship for aryl chlorides. From left to right: same ArCl as in Figure 3. (Free enthalpies in eV).
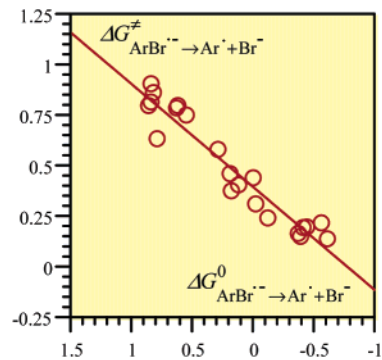
Figure 6. Activation/driving force relationship for aryl bromides. From left to right: same ArBr as in Figure 4. (Free enthalpies in eV).

mental $E^0_{ArX/ArX^{\bullet-}}$ that do not include the biphenyl derivatives. The present results (Figures 3–6) show that the correlations that include the biphenyl derivatives and use the experimental values of $E^0_{ArX/ArX^{\bullet-}}$ instead of the computed electron affinities have the same degree of scatter than those that exclude the biphenyl derivatives (correlation coefficient: 0.92 vs 0.92 for the chlorides, 0.96 vs 0.97 for the bromides). Still in connection with ref 11, we note that putting chlorides and bromides on the same plot would be justified only if there were reasons to a priori consider that the intrinsic barrier is the same in both cases,[20] whereas in fact we are aiming at deciphering the ingredients of this parameter.

It is remarkable that the slope of the correlation straight line is close to 0.5 in both cases (0.49 for the chlorides and 0.51 for the bromides). Since the driving force interval is spread out over both positive and negative values, a 0.5 slope suggests linearizing the quadratic activation/driving force relationship depicted by eq 1, thus leading to:

$$\Delta G^{\neq}_{ArX^{\bullet-} \rightarrow Ar^{\bullet}+X^-} = \Delta G^{\neq}_0 + 0.5\Delta G^0_{ArX^{\bullet-} \rightarrow Ar^{\bullet}+X^-}$$

The intrinsic barrier, $\Delta G^{\neq}_0$, is thus found as equal to 0.41 and 0.39 eV for the chlorides and bromides, respectively. This near equality is coincidental. Its implications in terms of bond bending effects will be discussed later on.

The intrinsic barrier predicted from eqs 3–5

$$\Delta G^{\neq}_0 = \frac{D_{ArX \rightarrow Ar^{\bullet}+X^{\bullet}} + E^0_{ArX/ArX^{\bullet-}} - E^0_{Ar^{\bullet}/[Ar^{\bullet}]^{\bullet-}} + \lambda_0}{4} \qquad (8)$$

may be estimated as follows. $E^0_{Ar^{\bullet}/[Ar^{\bullet}]^{\bullet-}}$ is likely to be close to

$E^0_{ArH/ArH^{\bullet-}}$. Furthermore, there is an approximate parallelism between $E^0_{ArH/ArH^{\bullet-}}$ and $E^0_{ArX/ArX^{\bullet-}}$. Therefore

$$E^0_{Ar^{\bullet}/[Ar^{\bullet}]^{\bullet-}} - E^0_{ArCl/ArCl^{\bullet-}} \cong -0.11 \pm 0.07 \text{ V}$$

and

$$E^0_{Ar^{\bullet}/[Ar^{\bullet}]^{\bullet-}} - E^0_{ArBr/ArBr^{\bullet-}} \cong -0.14 \pm 0.09 \text{ V}$$

The solvent reorganization energy, λ_0, is expected to be small as discussed elsewhere,[20,21] giving rise to a term $\lambda_0/4$ of the order of 0.15 and 0.1 eV for the chloro- and bromo- series, respectively. The predicted values of the intrinsic barrier are thus 1.23 and 1.03 eV for the chloro- and bromo-derivatives respectively, i.e., much larger than the experimental values.

There are two factors, not taken into account in the derivation of eqs 3–5, that contribute to lowering the barrier thus estimated. One is out-of-plane bending that allows avoidance of the conical intersection[12] encountered upon straight stretching of the carbon–halogen bond as in the model that underlies eqs 3–5. The other factor is that the cleavage of the π anion radical is likely to give rise to a weakly interacting cluster, that may be viewed equivalently as a σ anion radical, rather than to be strictly dissociative. Recent quantum chemical calculations have indeed shown the presence of such loose clusters on the potential energy profiles of several aryl chlorides and bromides.[11] As observed with several other organic halides these interactions may survive the presence of a polar solvent such as DMF.[22] Adaptation of previous Morse curve models,[8,22] shows that, in eq 4, the term $D_{ArX^{\bullet-}}$ should be replaced by $D_{ArX^{\bullet-}}(1 - \sqrt{D_{Ar^{\bullet},X^-}/D_{ArX^{\bullet-}}})^2$, where $D_{Ar^{\bullet},X^-}$ is the dissociation energy of the σ anion radical. We do not know the exact values of $D_{Ar^{\bullet},X^-}$, but we may note that even a small value of $D_{Ar^{\bullet},X^-}$ entails a strong decrease of the intrinsic barrier. For example, if $D_{Ar^{\bullet},X^-}$ were 4% of $D_{ArX^{\bullet-}}$, an intrinsic barrier of only 0.83 eV for chlorides and 0.67 eV for bromides would ensue.[23]

The other important accelerating factor, namely out-of-plane bending, may be introduced into the model under the same assumptions as in ref 12b, i.e., considering that the out-of-plane bending effect results from a compromise between the quadratic increase in energy required to bend the σ bond and the gain in resonance energy resulting from the lifting of the symmetry restriction. The first factor is assumed to follow an harmonic law, i.e., the energy increase varies as $(f/2)\theta^2$, where θ is the bending angle and f the force constant. The gain in resonance energy is assumed to be proportional to the bending angle: $H = h_0\theta$. It follows (see Supporting Information) that eq 1 remains valid but with a different definition of the intrinsic barrier. This is now given by eq 9, which replaces eq 8.

(20) The same remark also applies to Figure 7 in ref 5g.
(21) Costentin, C.; Robert, M.; Savéant, J.-M. *J. Am. Chem. Soc.* **2003**, *125*, 105.
(22) (a) Cardinale, A.; Gennaro, A.; Isse, A. A.; Maran, F. In *New Directions in Organic Electrochemistry*; Fry, A. J., Matsumura, A., Eds.; The Electrochemical Society, Inc.: New Jersey, 2000; Vol. 200–15, pp 136–140. (b) Pause, L.; Robert, M.; Savéant, J.-M. *J. Am. Chem. Soc.* **2000**, *122*, 9829. (c) Pause, L.; Robert, M.; Savéant, J.-M. *J. Am. Chem. Soc.* **2001**, *123*, 11908–11916. (d) Cardinale, A.; Isse, A. A.; Gennaro, A.; Robert, M.; Savéant, J.-M. *J. Am. Chem. Soc.* **2002**, *124*, 13533.
(23) Note that taking into account the effect of the σ anion radical produces a lowering of the barrier that is similar, although not idendical, to the modification of the classical Morse purely dissociative model by introduction of a dissociative product curve smoother than the repulsive part of the reactant Morse curve.[12b]

$$\Delta G_0^{\neq} = \frac{\lambda_0 + (\sqrt{D_{ArX^{\bullet-}}} - \sqrt{D_{Ar,X^-}})^2}{4} - \frac{h_0^2}{2f} \quad (9)$$

$h_0^2/2f$ may be regarded as constant within the linearized region around the zero of driving force. After linearization, the activation-driving force relationship writes

$$\Delta G_{ArX^{\bullet-} \to Ar^{\bullet}+X^-}^{\neq} = \frac{\lambda_0 + (\sqrt{D_{ArX^{\bullet-}}} - \sqrt{D_{Ar,X^-}})^2}{4} - \frac{h_0^2}{2f} + 0.5\Delta G_{ArX^{\bullet-} \to Ar^{\bullet}+X^-}^0 \quad (10)$$

Replacement of eq 7 by eq 10 amounts to a decrease of the intrinsic barrier through two terms, $-h_0^2/2f$ and $\sqrt{D_{Ar^{\bullet},X^-}}$. The various ingredients of this estimate of the intrinsic barrier may not be derived from experimental data, making necessary the recourse to quantum chemical calculations. In this respect, values of $h_0^2/2f$ comprised between 0.3 and 0.5 eV, as recently computed for 4-cyanochlorobenzene,[12] seem quite compatible with the experimental data gathered in Figures 5 and 6 for the chloro and bromo series, respectively.

Comparison of the two series indicate that the avoided conical intersection energy, $h_0^2/2f$, is larger for chlorides than for bromides. The experimental intrinsic barriers are indeed about the same while the corrected bond dissociation energy, $(\sqrt{D_{ArX^{\bullet-}}} - \sqrt{D_{Ar^{\bullet},X^-}})^2$ is larger for chlorides than for bromides, the difference being compensated by a value of $h_0^2/2f$ stronger in the first case than in the second. This observation can be rationalized by noting that bending the bond should be more difficult with Br than with Cl because of a better overlap of one of the halogen nonbonding p orbitals with the π ring system.

With or without inclusion of the biphenyl derivatives, the correlations show substantial scatter. What are the possible causes of the ensuing inference that they do not reproduce well the consequences of small structural changes? One of these is likely to be the bond bending effect. $h_0^2/2f$ may indeed vary significantly from one isomer to the other within the same family of halides. This is not however the sole possible source of scatter. Interactions between caged fragments may vary as well. This is also the case of the degree of validity of the two assumptions made to justify the existence of the correlations, namely taking $E^0_{Ar^{\bullet}/[Ar^{\bullet}]^{\bullet-}}$ as equal to $E^0_{ArH/ArH^{\bullet-}}$ and of the parallelism between $E^0_{ArH/ArH^{\bullet-}}$ and $E^0_{ArX/ArX^{\bullet-}}$.

Concluding Remarks

Recent rate data obtained by pulse radiolysis for very fast cleaving of aryl chloride and bromide anion radicals can be accommodated in a correlation between fragmentation rate constant and ArX/ArX$^{\bullet-}$ standard potential. The correlation holds after inclusion of these new data provided the standard potential are determined experimentally. Cyclic voltammetry is used for this purpose, taking due account of the mixed character the electron transfer/fragmentation reaction kinetics. Activation/driving force linear plots may thus be derived with an estimation of the driving force based on experimental data. The ensuing intrinsic barriers are of the order of 0.4 eV for both the chloride and bromide series. Application of the classical Morse-curve model of these intramolecular dissociative electron transfer reactions leads to substantially higher values. Improvement of the model by taking into account the possible formation

of a σ anion radical and, above all, of the avoiding of a conical intersection by bending the cleaving bond allows a satisfactory rationalization of the existing data.

Experimental Section

Chemicals. *N*, *N*-dimethylformamide (Fluka, > 99.5%, stored on molecular sieves and under argon atmosphere), 1-methyl-2-pyrrolidinone (Aldrich, 99.5%, anhydrous), the supporting electrolyte Bu_4BF_4 (Fluka, puriss), 2-chlorobiphenyl (Aldrich, 99.9%), 3-chlorobiphenyl (Aldrich, 98.7%), 4-chlorobiphenyl (Aldrich, 99.4%), 2-bromobiphenyl (Aldrich, 96%), 3-bromobiphenyl (Aldrich, 97%), 4-bromobiphenyl (Aldrich, 98%) were used as received.

Instrumentation. The working electrode was a 3 mm-diameter glassy carbon electrode disk (Tokai) carefully polished and ultrasonically rinsed in absolute ethanol before use. The counter-electrode was a platinum wire and the reference electrode an aqueous SCE electrode. The potentiostat, equipped with a positive feedback compensation and current measurer, used at low or moderate scan rates, was the same as previously described.[24] All experiments have been done at 22 °C, the double-wall jacket cell being thermostated by circulation of water.

Quantum Chemical Calculation Methodology. All the calculations were performed with the Gaussian 98 series of programs.[25] DFT (B3P86) method and 6-311++G** basis set were used. Minimum

energy structures were fully optimized. Frequency calculations were made to verify that the structures were minima (no imaginary frequencies) and to evaluate thermodynamic functions. The bond dissociation energies were derived from the procedure described in ref 25 with an empirical correction aiming at a satisfactory reproduction of experimental data.[26]

Supporting Information Available: (i) Extraction of the standard potential $E^0_{ArX/ArX^{\bullet-}}$ from the cyclic voltammetric data for the chloro and bromo-biphenyls. (ii) Establishment of eq 9. This material is available free of charge via the Internet at http://pubs.acs.org.

(24) Garreau, D.; Savéant, J.-M. *J. Electroanal. Chem*. **1972**, *35*, 309.

(25) Frisch, M. J.; Trucks, G. W.; Schlegel, H. B.; Scuseria, M. A.; Gill, P. M. W.; Johnson, B. G.; Robb, M. A.; Cheeseman, J. R.; Keith, T.; Petersson, G. A.; Montgomery, Stratmann, R. E.; Burant, J. C.; Dapprich, S.; Millam, J. M.; Daniels, A. D.; Kudin, K. N.; Strain, M. C.; Farkas, O.; Tomasi, J.; Barone, V.; Cossi, M.; Cammi, R.; Mennuci, B.; Pomelli, C.; Adamo, C.; Clifford, S.; Ochterski, G.; Cui, Q.; Morokuma, K.; Malick, D. K.; Rabuck, A. D.; J. A.; Raghavachari, K.; Al-Laham, M. A.; Zakrzewski, V. G.; Ortiz, J. V.; Foresman, J. B.; Cioslowski, J.; Stefanov, B. B.; Liu, G.; Liashenko, A.; Piskorz, P.; Komaromi, I.; Nanayakkara, A.; Challacombe, M.; Peng, C. Y.; Ayala, P. Y.; Chen, W.; Wong, M. W.; Andres, J. L.; Replogle, A. S.; Gomperts, R.; Martin, R. L.; Fox, D. J.; Binkley, J. S.; Defrees, D. J.; Baker, J.; Stewart, J. P.; Head-Gordon, M.; Gonzalez, C.; Pople, J. A. *Gaussian 98*, Revision A.1; Gaussian, Inc.: Pittsburgh, PA, 1998.

(26) Lazarou, Y. G.; Prosmitis, A. V.; Papadimitriou, V. C.; Papagiannakopoulos, P. *J. Phys Chem. A* **2001**, *105*, 6729.